Chapter 1
Thermodynamics of Molecular Liquids in Random Porous Media: Scaled Particle Theory and the Generalized Van der Waals Equation

Myroslav Holovko, Volodymyr Shmotolokha and Taras Patsahan

Abstract A new approach to the theoretical description of molecular liquids confined in random porous media is proposed in order to study their thermodynamic properties. The models applied in our study are characterized by the intermolecular interactions consisting of repulsive and attractive parts, both of which are of the anisotropic nature. To take into account an anisotropy of the repulsion the scaled particle theory (SPT) is extended for the system of a hard convex body (HCB) fluid in a quenched matrix of hard particles forming a random porous medium. A contribution of the anisotropic attractive interaction is considered on the level of the mean-field or Van der Waals approximation. Therefore, combining the obtained analytical results within the framework of the perturbation theory the equation of state for confined liquids is derived. On the basis of the developed approach we can consider a fluid in a random matrix using various models. A reliability of the SPT theory is proved on the examples of hard sphere and hard spherocylinder fluids in different matrices. For a spherocylinder fluid with attractive intermolecular interaction the phase transition diagrams are constructed to study a vapour-liquid-nematic equilibrium and the effect of confinement on it. It is shown that a matrix porosity decrease leads to decreasing of the critical temperature and the critical density of vapour-liquid phase transition. In the case of long spherocylinders ($L_1/D_1 = 10$) the vapour-liquid transition of a fluid in a matrix can disappear completely being suppressed by the isotropic-nematic phase transition. On the other hand the coexistence between vapour and nematic phases is observed for a spherocylinder fluid at the conditions comparable to the Onsager limit

M. Holovko (✉) · V. Shmotolokha · T. Patsahan
Institute for Condensed Matter Physics of the National Academy of Sciences of Ukraine,
1 Svientsitskii Str, Lviv 79011, Ukraine
e-mail: holovko@icmp.lviv.ua

V. Shmotolokha
e-mail: shmotolokha@icmp.lviv.ua

T. Patsahan
e-mail: tarpa@icmp.lviv.ua

L. Bulavin and N. Lebovka (eds.), *Physics of Liquid Matter: Modern Problems*,
Springer Proceedings in Physics 171, DOI 10.1007/978-3-319-20875-6_1

($L_1/D_1 = 80$). The anisotropy of attractive potential causes the broadening of the liquid-nematic coexistence region and in the case of essentially high rates of anisotropy the vapour-liquid transition vanishes. It is noticed that the presence of porous medium enhances this effect. The presented review is aimed to illustrate an application of the SPT approach which developed recently for fluids of non-spherical molecules confined in random porous media.

1.1 Introduction

Many different materials such as silicas and zeolites, activated carbons and clays, cements and ceramics, metal foams and others can be considered as porous media. Molecular fluids confined in such porous materials with pore sizes ranging from a few nanometers to hundreds nanometers can undergo drastic modifications in their physical and physicochemical properties. For example, it is well established that confinement can induce drastic shifts of phase equilibria, e.g. narrowing of the vapour-liquid coexistence curve, lowering of the pore critical temperature, decreasing of the critical density and the appearance of new types of phase transitions, which are not observed in the bulk [1]. Besides its fundamental interest, a thorough understanding of the influence of confinement on the physical and chemical properties of fluids is highly useful in many areas of applied science and engineering, geosciences, biophysics, material science etc. Different porous materials are widely used in the chemical, oil and gas, food and pharmaceutical industries for pollution control, mixture separation, and as catalyst or catalyst support for chemical reactions. In parallel with experimental studies a lot of different molecular models were introduced for the investigation of the properties of fluids in porous media within the framework of computer simulations and theoretical approaches. Atomistic molecular simulations methods have been widely used to characterize adsorption in porous materials [2, 3], including the structure and dynamics of adsorbed phases, thermodynamics of adsorption, the influence of structural heterogeneity of pores and chemical heterogeneity of pore surface [4, 5], the influence of porous media on the isotropic-nematic phase transition like in confined liquid crystals fluids [6, 7]. Also numerous computer simulation studies have been devoted to the same problems, but in isolated pores of slit-like or cylindrical shapes. Theoretical approaches used for the description of fluids in porous media are mostly based on the method of Ornstein-Zernike equations [8–11] and the method of density functional theory [12, 13]. In the present review we consider fluids confined in porous materials with a random or disordered structure, in which pores are formed by randomly distributed solid particles. In these materials the pore shapes and sizes are not well defined, they are not isolated but build a network with very complex topology. The systems of such a kind cannot be described by a single pore model, thus in theoretical approaches as well as in computer simulations one should take into account the whole variety of statistically probable configurations of pores.

Much theoretical efforts have been devoted within the framework of statistical mechanical methods to a study of fluids in random porous media during the last three decades starting from the pioneering work of Madden and Gland [8]. In this work a porous medium is presented as a quenched configuration of randomly distributed spherical particles that form so-called matrix [8]. The specific of description of fluids in such porous media is connected with the double quenched-annealed averages: the annealed average is taken over all fluid configurations and the additional quenched average should be taken over all realizations of the matrix. One standard approach to solve this problem is based on the replica method. It consists in the description of a fluid in a random porous medium as the $(s+1)$ component equilibrium mixture of a matrix and s replicated copies of a fluid, which do not interact with each other, and then the limit $s \to 0$ is to be taken. Using the replica Ornstein-Zernike (ROZ) integral equation theory [9], the statistical mechanics approach of liquid state was extended to a description of different models of a fluid confined in random porous matrices [14, 15] including the chemical reacting fluids adsorbed in porous media [16, 17]. However, unlike bulk fluids, no analytical result have been obtained from the ROZ integral equations approach even for the simplest model such as a hard-sphere fluid in a hard sphere matrix.

The first rather accurate analytical results for a hard sphere fluid in hard-sphere (HS) and overlapping hard-sphere (OHS) matrices were obtained quite recently [18–20] by extending the classic scaled particle theory (SPT) [21–23]. The SPT approach is based on a combination of the exact treatment of a point scaled particle in a HS fluid with the thermodynamic consideration of a finite size scaled particle. The exact result for a point scaled particle in a HS fluid confined in a random matrix was obtained in [18]. However, the approach proposed in [18] and named as SPT1 contains a subtle inconsistency appearing when a size of matrix particles is essentially larger than a size of fluid particles. Later, this inconsistency was eliminated in a new approach named as SPT2 [20].

The expressions obtained in SPT2 include two types of porosities. One of them is defined by a pure geometry of porous medium (geometrical porosity ϕ_0 characterizing the free volume for a fluid) and the second one is defined by the chemical potential of a fluid in the limit of infinite dilution (probe particle porosity ϕ characterizing the adsorption of a fluid in an empty matrix). On the basis of SPT2 approach the approximation SPT2b was proposed, and it was shown that it reproduces the computer simulation data with a very good accuracy at small and intermediate fluid densities. However, the expressions obtained in the SPT2 and SPT2b approximations contain a divergence at the packing fraction of fluid equal to the probe particle porosity ϕ. Consequently, the prediction of thermodynamic properties at high densities of a fluid can be inaccurate, especially when it reaches close packing conditions. An accuracy of SPT2 and SPT2b approximations also becomes worse when fluid and matrix particles are of comparable sizes [20]. Later, in the investigation of one-dimensional hard rode fluid in a random porous medium [24] a series of the new approximations SPT2b1, SPT2b2 and SPT2b3 were proposed, which are free of the mentioned drawbacks. Two last approximations

contain the third type of porosity ϕ^* defined by the maximum value of packing fraction of fluid in a porous medium. It was shown that these new approximations essentially improve the SPT predictions at high fluid densities. The application of the SPT theory and generalization of the SPT2b1 approximation to the case of HS fluid confined in random matrices were reviewed recently in [25], where thermodynamic properties of fluid were calculated. A comparison of obtained results with computer simulation data proved applicability and high reliability of the SPT for the wide range of fluid densities and different matrix parameters.

A remarkable feature of the SPT theory is a possibility of its generalization for the description of non-spherical hard convex body fluids in the bulk, which can be done using one [26, 27] and two [28] scaling parameters. The SPT theory can also be applied for the description of nematic ordering in hard convex body (HCB) fluids [28–30]. Recently, the SPT theory was extended for HCB fluids confined in random matrix [31]. The generalization of the SPT theory for a HCB fluid confined in a random porous medium with a use of two scaling parameters was presented, and the effect of porous media on the orientational ordering in a HCB fluid was studied [32].

In this chapter the extension of SPT theory for the description of thermodynamic properties of non-spherical molecular fluids confined in random porous media is reviewed. First we present the generalization of SPT theory for a HCB fluid in random porous media. Then we consider the SPT theory with two scaling parameters for the description of a hard spherocylinder fluid in a random matrix. After that a system of hard spherocylinders in a matrix is used as the reference system [33, 34] in the generalization of Van der Waals equation for anisotropic fluids confined in random porous media. Finally, the derived equations are applied to investigate the effect of porous media on the vapour-liquid-nematic phase equilibria in molecular fluids.

1.2 HCB Fluids in Random Porous Media: SPT with One Scaling Parameter

Hard convex body (HCB) particles are characterized by three geometrical parameters—the volume V, the surface area S and the mean curvature R with a factor $1/4\pi$. For example, for a frequently considered case of a system of spherocylindrical rods with the length L and the diameter D, these parameters are

$$V = \frac{1}{4}\pi D^2 L + \frac{1}{6}\pi D^3, \quad S = \pi DL + \pi D^2, \quad R = \frac{1}{4}L + \frac{1}{2}D. \tag{1.1}$$

The basic idea of the SPT approach is an insertion of an additional scaled particle of a variable size into a fluid. To this aim we introduce the scaling parameter λ_s in such a way that the volume V_s, the surface area S_s and the curvature R_s of scaled particle are modified as

$$V_s = \lambda_s^3 V_1, \quad S_s = \lambda_s^2 S_1, \quad R_s = \lambda_s R_1, \tag{1.2}$$

where V_1, S_1 and R_1 are the volume, the surface area and the mean curvature of a fluid particle respectively. Hereafter, we use the conventional notations [9, 14, 15], where the index "1" is used to denote fluid component and the index "0" denotes matrix particles. For scaled particles the index "s" is used.

Procedure of insertion of the scaled particle into a fluid is equivalent to a creation of cavity, which is free of any other fluid particles. The key point of considered reformulation of the SPT theory consists in a derivation of the excess chemical potential of a scaled particle μ_s^{ex}, which is equal to a work needed to create the corresponding cavity. In the presence of a porous medium the expression of excess chemical potential for a small scaled particle in a HCB fluid can be written in the form

$$\begin{aligned}\beta\mu_s^{ex} = \beta\mu_s - \ln(\rho_1 \Lambda_1^3 \Lambda_{1R}) = \ln p_0(\lambda_s) \\ - \ln\left[1 - \frac{\eta_1}{p_0(\lambda_s)}\left(1 + 3\lambda_s\alpha_1 + 3\lambda_s^2\alpha_1 + \lambda_s^3\right)\right],\end{aligned} \tag{1.3}$$

where $\beta = 1/(k_B T)$, k_B is the Boltzmann constant, T is the temperature, $\eta_1 = \rho_1 V_1$ is the fluid packing fraction, ρ_1 is the fluid density, Λ_1 is the fluid thermal wave length, the quantity Λ_{1R}^{-1} is the rotational partition function of a single molecule [35], and $\alpha_1 = \frac{R_1 S_1}{3V_1}$ is the non-sphericity parameter of a fluid particle. The term $p_0(\lambda_s) = \exp(-\beta\mu_s^0)$ is defined by the excess chemical potential of the scaled particle confined in an empty matrix μ_s^0, and it has a meaning of probability to find a cavity created by the scaled particle in the matrix in the absence of fluid particles.

For the large scaled particle the excess chemical potential is given by the thermodynamical expression for the work needed to create a macroscopic cavity inside a fluid confined in a porous medium. It can be presented as follows

$$\beta\mu_s^{ex} = w(\lambda_s) + \frac{\beta P V_s}{p_0(\lambda_s)}, \tag{1.4}$$

where P is the pressure of fluid, V_s is the volume of scaled particle. The multiplier $1/p_0(\lambda_s)$ appears due to an excluded volume occupied by matrix particles, which can be considered as a probability to find a cavity created by a scaled particle in the matrix in the absence of fluid particles. This probability is related directly to two different types of the porosities [20]. The first one corresponds to the case of $\lambda_s = 0$ and gives the geometrical porosity

$$\phi_0 = p_0(\lambda_s = 0), \tag{1.5}$$

which depends only on a structure of matrix and it is related to the volume of a void between matrix particles. The second type of porosity corresponds to the case of $\lambda_s = 1$ and gives the probe particle porosity [20]

$$\phi = p_0(\lambda_s = 1), \tag{1.6}$$

which is defined by the excess chemical potential of a fluid in the limit of infinite dilution μ_1^0. Thus, it depends also on a nature of fluid under study.

According to the ansatz of the SPT theory [18–25], $w(\lambda_s)$ can be presented in the form of expansion

$$w(\lambda_s) = w_0 + w_1\lambda_s + \frac{1}{2}w_2\lambda_s^2. \tag{1.7}$$

The coefficients of this expansion can be found from the continuity of μ_s^{ex} and its corresponding derivatives $\partial\mu_s^{ex}/\partial\lambda_s$ and $\partial^2\mu_s^{ex}/\partial\lambda_s^2$ at $\lambda_s = 0$. Consequently, one derives the following expressions [25–31]:

$$\begin{aligned} w_0 &= -\ln(1-\eta_1/\phi_0), \\ w_1 &= \frac{\eta_1/\phi_0}{1-\eta_1/\phi_0}\left(3\alpha_1 - \frac{p_0'}{\phi_0}\right), \\ w_2 &= \frac{\eta_1/\phi_0}{1-\eta_1/\phi_0}\left[6\alpha_1 - 6\alpha_1\frac{p_0'}{\phi_0} + 2\left(\frac{p_0'}{\phi_0}\right)^2 - \frac{p_0''}{\phi_0}\right] \\ &\quad + \left(\frac{\eta_1/\phi_0}{1-\eta_1/\phi_0}\right)^2\left(3\alpha_1 - \frac{p_0'}{\phi_0}\right)^2, \end{aligned} \tag{1.8}$$

where $p_0' = \frac{\partial p_0(\lambda_s)}{\partial\lambda_s}$ and $p_0'' = \frac{\partial^2 p_0(\lambda_s)}{\partial\lambda_s^2}$ at $\lambda_s = 0$.

After setting $\lambda_s = 1$ the expression (1.4) leads to the relation between the pressure P and the excess chemical potential μ_1^{ex} of a fluid in a matrix

$$\begin{aligned} \beta\left(\mu_1^{ex} - \mu_1^0\right) &= -\ln(1-\eta_1/\phi_0) + A\frac{\eta_1/\phi_0}{1-\eta_1/\phi_0} + B\frac{(\eta_1/\phi_0)^2}{(1-\eta_1/\phi_0)^2} \\ &\quad + \frac{\beta P}{\rho_1}\frac{\eta_1}{\phi}, \end{aligned} \tag{1.9}$$

where the coefficients A and B define the porous medium structure and the expressions for them are as follow:

$$\begin{aligned} A &= 3\alpha_1 - \frac{p_0'}{\phi_0} + \frac{1}{2}\left[6\alpha_1 - 6\frac{p_0'}{\phi_0}\alpha_1 + 2\left(\frac{p_0'}{\phi_0}\right)^2 - \frac{p_0''}{\phi_0}\right], \\ B &= \frac{1}{2}\left(3\alpha_1 - \frac{p_0'}{\phi_0}\right)^2. \end{aligned} \tag{1.10}$$

Using the Gibbs-Duhem equation

$$\left(\frac{\partial P}{\partial \rho_1}\right)_T = \rho_1 \left(\frac{\partial \mu_1}{\partial \rho_1}\right)_T \tag{1.11}$$

one derives the fluid compressibility

$$\begin{aligned}\beta\left(\frac{\partial P}{\partial \rho_1}\right)_T = & \frac{1}{(1-\eta_1/\phi)} + (1+A)\frac{\eta_1/\phi_0}{(1-\eta_1/\phi)(1-\eta_1/\phi_0)} \\ & + (A+2B)\frac{(\eta_1/\phi_0)^2}{(1-\eta_1/\phi)(1-\eta_1/\phi_0)^2} \\ & + 2B\frac{(\eta_1/\phi_0)^3}{(1-\eta_1/\phi)(1-\eta_1/\phi_0)^3},\end{aligned} \tag{1.12}$$

which makes it possible to obtain the total chemical potential, $\beta\mu_1 = \ln(\rho_1 \Lambda_1^3 \Lambda_{1R}) + \beta\mu_1^{ex}$, and the pressure of a fluid, and a result of integration of (1.12) over the fluid density leads to [31]:

$$\begin{aligned}\beta(\mu_1^{ex} - \mu_1^0) = & -\ln(1-\eta_1/\phi) + (A+1)\frac{\phi}{\phi-\phi_0}\ln\frac{1-\eta_1/\phi}{1-\eta_1/\phi_0} \\ & + (A+2B)\frac{\phi}{\phi-\phi_0}\left(\frac{\eta_1/\phi_0}{1-\eta_1/\phi_0} - \frac{\phi}{\phi-\phi_0}\ln\frac{1-\eta_1/\phi}{1-\eta_1/\phi_0}\right) \\ & + 2B\frac{\phi}{\phi-\phi_0}\left[\frac{1}{2}\frac{(\eta_1/\phi_0)^2}{(1-\eta_1/\phi_0)^2} - \frac{\phi}{\phi-\phi_0}\frac{\eta_1/\phi_0}{1-\eta_1/\phi_0}\right. \\ & \left. + \frac{\phi^2}{(\phi-\phi_0)^2}\ln\frac{1-\eta_1/\phi}{1-\eta_1/\phi_0}\right],\end{aligned} \tag{1.13}$$

$$\begin{aligned}\frac{\beta P}{\rho_1} = & -\frac{\phi}{\eta_1}\ln\frac{1-\eta_1/\phi}{1-\eta_1/\phi_0} + (1+A)\frac{\phi}{\eta_1}\frac{\phi}{\phi-\phi_0}\ln\frac{1-\eta_1/\phi}{1-\eta_1/\phi_0} \\ & + (A+2B)\frac{\phi}{\phi-\phi_0}\left[\frac{1}{1-\eta_1/\phi_0} - \frac{\phi}{\eta_1}\frac{\phi}{\phi-\phi_0}\ln\frac{1-\eta_1/\phi}{1-\eta_1/\phi_0}\right] \\ & + 2B\frac{\phi}{\phi-\phi_0}\left[\frac{1}{2}\frac{\eta_1/\phi_0}{(1-\eta_1/\phi_0)^2} - \frac{2\phi-\phi_0}{\phi-\phi_0}\frac{1}{1-\eta_1/\phi_0}\right. \\ & \left. + \frac{\phi}{\eta_1}\frac{\phi^2}{(\phi-\phi_0)^2}\ln\frac{1-\eta_1/\phi}{1-\eta_1/\phi_0}\right].\end{aligned} \tag{1.14}$$

The expressions (1.13) and (1.14) are the result of SPT2 approach. At high fluid densities the obtained expressions have two divergences, which appear in $\eta_1 = \phi$ and $\eta_1 = \phi_0$ respectively. Since $\phi < \phi_0$ the first divergence in $\eta_1 = \phi$ occurs at lower densities than the second one. From geometrical point of view such a divergence should appear at higher densities close to the maximum value of fluid

packing fraction $\eta_1^{\max}$ available for a fluid in a given matrix. The different corrections and improvements of the SPT2 approach were proposed in [20, 24, 25, 31]. First corrections were given in [20], where on the basis of SPT2 four approximations were developed. One of them called SPT2b can be derived if ϕ is replaced by ϕ_0 everywhere in (1.12) except the first term. As a result, (1.13) and (1.14) can be rewritten in the following form

$$\begin{aligned}\beta\left(\mu_1^{ex}-\mu_1^0\right)^{SPT2b} &= -\ln(1-\eta_1/\phi)+(1+A)\frac{\eta_1/\phi_0}{1-\eta_1/\phi_0}\\ &+\frac{1}{2}(A+2B)\frac{(\eta_1/\phi_0)^2}{(1-\eta_1/\phi_0)^2}+\frac{2}{3}B\frac{(\eta_1/\phi_0)^3}{(1-\eta_1/\phi_0)^3},\end{aligned} \tag{1.15}$$

$$\begin{aligned}\left(\frac{\beta P}{\rho_1}\right)^{SPT2b} &= -\frac{\phi}{\eta_1}\ln\left(1-\frac{\eta_1}{\phi}\right)+\frac{\phi_0}{\eta_1}\ln\left(1-\frac{\eta_1}{\phi_0}\right)+\frac{1}{1-\eta_1/\phi_0}\\ &+\frac{A}{2}\frac{\eta_1/\phi_0}{(1-\eta_1/\phi_0)^2}+\frac{2B}{3}\frac{(\eta_1/\phi_0)^2}{(1-\eta_1/\phi_0)^3}.\end{aligned} \tag{1.16}$$

The second approximation proposed in [24, 25] is called SPT2b1 and it corrects SPT2b by removing the divergence at $\eta_1=\phi$ through an expansion of the logarithmic term in (1.15)

$$-\ln(1-\eta_1/\phi)\approx-\ln(1-\eta_1/\phi_0)+\frac{\eta_1(\phi_0-\phi)}{\phi_0\phi(1-\eta_1/\phi_0)}. \tag{1.17}$$

Therefore, one obtains the expressions for the chemical potential and pressure within the SPT2b1 approximation as follows

$$\begin{aligned}\beta\left(\mu_1^{ex}-\mu_1^0\right)^{SPT2b1} &= -\ln(1-\eta_1/\phi_0)+(1+A)\frac{\eta_1/\phi_0}{1-\eta_1/\phi_0}+\frac{\eta_1(\phi_0-\phi)}{\phi_0\phi(1-\eta_1/\phi_0)}\\ &+\frac{1}{2}(A+2B)\frac{(\eta_1/\phi_0)^2}{(1-\eta_1/\phi_0)^2}+\frac{2}{3}B\frac{(\eta_1/\phi_0)^3}{(1-\eta_1/\phi_0)^3},\end{aligned} \tag{1.18}$$

$$\begin{aligned}\left(\frac{\beta P}{\rho_1}\right)^{SPT2b1} &= \frac{1}{1-\eta_1/\phi_0}\frac{\phi_0}{\phi}+\left(\frac{\phi_0}{\phi}-1\right)\frac{\phi_0}{\eta_1}\ln\left(1-\frac{\eta_1}{\phi_0}\right)\\ &+\frac{A}{2}\frac{\eta_1/\phi_0}{(1-\eta_1/\phi_0)^2}+\frac{2B}{3}\frac{(\eta_1/\phi_0)^2}{(1-\eta_1/\phi_0)^3}.\end{aligned} \tag{1.19}$$

Two other approximations called SPT2b2 and SPT2b3 contain the third type of porosity ϕ^* defined by the maximum value of packing fraction of a fluid in a porous medium and provide the more correct description of thermodynamic properties of a fluid in the high-density region, which corresponds to the close packing condition.

To introduce ϕ^* in the expression for the chemical potential (1.15) the logarithmic term is modified in the following way

$$-\ln(1-\eta_1/\phi) \approx -\ln(1-\eta_1/\phi^*) + \frac{\eta_1(\phi^*-\phi)}{\phi^*\phi(1-\eta_1/\phi^*)}. \tag{1.20}$$

Consequently, the SPT2b2 approximation is derived as

$$\begin{aligned}\beta\left(\mu_1^{ex}-\mu_1^0\right)^{SPT2b2} &= -\ln(1-\eta_1/\phi^*) + \frac{\eta_1/\phi_0}{1-\eta_1/\phi_0}(1+A) \\ &+ \frac{\eta_1(\phi^*-\phi)}{\phi^*\phi(1-\eta_1/\phi^*)} + \frac{1}{2}(A+2B)\frac{(\eta_1/\phi_0)^2}{(1-\eta_1/\phi_0)^2} + \frac{2}{3}B\frac{(\eta_1/\phi_0)^3}{(1-\eta_1/\phi_0)^3},\end{aligned} \tag{1.21}$$

$$\begin{aligned}\left(\frac{\beta P}{\rho_1}\right)^{SPT2b2} &= -\frac{\phi^*}{\eta_1}\ln\left(1-\frac{\eta_1}{\phi^*}\right) + \frac{\phi_0}{\eta_1}\ln\left(1-\frac{\eta_1}{\phi_0}\right) + \frac{1}{1-\eta_1/\phi_0} \\ &+ \frac{\phi^*-\phi}{\phi}\left[\ln(1-\eta_1/\phi^*) + \frac{\eta_1/\phi^*}{1-\eta_1/\phi^*}\right]. \\ &+ \frac{A}{2}\frac{\eta_1/\phi_0}{(1-\eta_1/\phi_0)^2} + \frac{2}{3}B\frac{(\eta_1/\phi_0)^2}{(1-\eta_1/\phi_0)^3}.\end{aligned} \tag{1.22}$$

Finally, the SPT2b3 approximation can be obtained similar to the SPT2b2 approximation through an expansion of the logarithmic term $\ln(1-\eta_1/\phi^*)$ in the expression (1.21) for the chemical potential. As a result we obtain

$$\begin{aligned}\beta\left(\mu_1^{ex}-\mu_1^0\right)^{SPT2b3} &= -\ln(1-\eta_1/\phi_0) + \frac{\eta_1/\phi^*}{1-\eta_1/\phi_0} + \frac{\eta_1(\phi^*-\phi)}{\phi^*\phi(1-\eta_1/\phi^*)} \\ &+ A\frac{\eta_1/\phi_0}{1-\eta_1/\phi_0} + \frac{1}{2}(A+2B)\frac{(\eta_1/\phi_0)^2}{(1-\eta_1/\phi_0)^2} + \frac{2}{3}B\frac{(\eta_1/\phi_0)^3}{(1-\eta_1/\phi_0)^3},\end{aligned} \tag{1.23}$$

$$\begin{aligned}\left(\frac{\beta P}{\rho_1}\right)^{SPT2b3} &= \frac{\phi^*-\phi}{\phi}\left[\ln\left(1-\frac{\eta_1}{\phi^*}\right) + \frac{\eta_1/\phi^*}{1-\eta_1/\phi^*}\right] + \frac{1}{1-\eta_1/\phi_0} \\ &+ \frac{\phi_0-\phi^*}{\phi^*}\left[\ln(1-\eta_1/\phi_0) + \frac{\eta_1/\phi_0}{1-\eta_1/\phi_0}\right] \\ &+ \frac{A}{2}\frac{\eta_1/\phi_0}{(1-\eta_1/\phi_0)^2} + \frac{2}{3}B\frac{(\eta_1/\phi_0)^2}{(1-\eta_1/\phi_0)^3}.\end{aligned} \tag{1.24}$$

In [24] it was shown on the example of one-dimensional system of a fluid in a random matrix that ϕ^* is related to ϕ_0 and ϕ with the following relation

$$1/\phi^* = (1/\phi - 1/\phi_0)/\ln(\phi_0/\phi). \tag{1.25}$$

Since (1.25) is presented in the general form and does not depend directly on the dimensionality of the system, we extend its application to the three-dimensional case. In the bulk all the porosities are equal $\phi = \phi_0 = \phi^* = 1$. Therefore, the expressions for pressure and chemical potential of bulk hard sphere (HS) and HCB fluids have the same divergence at $\eta_1 = 1$ [33, 34]. In the case of a fluid in a porous medium one gets an inequality $\phi < \phi^* < \phi_0$. It should be noted that in the case when matrix particles size is essentially larger than a size of fluid particles, i.e. a size ratio of fluid to matrix particles tends to zero, hence the porosities tend to the same value $\phi \approx \phi_0 \approx \phi^*$ and all the considered approximations lead to the same result, which is equivalent to a bulk fluid with the effective density $\hat{\eta}_1 = \eta_1/\phi_0$.

An application of the developed theory is illustrated for two models of porous medium in [31]. The first model is a HCB matrix and the second model is an overlapping hard convex body (OHCB) matrix. The geometrical porosities for these models have the form [31]

$$\phi_0 = 1 - \eta_0 \tag{1.26}$$

for a HCB matrix and

$$\phi_0 = \mathrm{e}^{-\eta_0} \tag{1.27}$$

for an OHCB matrix, where $\eta_0 = \rho_0 V_0$, $\rho_0 = \frac{N_0}{V}$, N_0 is the number of matrix particles, V_0 is the volume of a matrix particle and V is the total volume of system.

Using the SPT theory [27] the following expression for the probe particle porosity ϕ is derived

$$\begin{aligned}\phi = e^{-\beta\mu_1^0} = (1-\eta_0)\exp\Bigg[-\Bigg(\frac{\eta_0}{1-\eta_0}\Bigg(3\alpha_0\Bigg(\frac{R_1}{R_0}+\frac{S_1}{S_0}\Bigg)+\frac{V_1}{V_0}\Bigg)\\ +\frac{3\alpha_0\eta_0^2}{2(1-\eta_0)^2}\Bigg(3\alpha_0\frac{R_1^2}{R_0^2}+2\frac{V_1}{V_0}\Bigg)+\frac{3\alpha_0^2\eta_0^3}{(1-\eta_0)^3}\frac{V_1}{V_0}\Bigg)\Bigg]\end{aligned} \tag{1.28}$$

for the case of a HCB matrix and

$$\phi = e^{-\beta\mu_1^0} = \exp\Bigg[-\eta_0\Bigg(1+3\alpha_0\frac{R_1}{R_0}+3\alpha_0\frac{S_1}{S_0}+\frac{V_1}{V_0}\Bigg)\Bigg] \tag{1.29}$$

for the case of an OHCB matrix, where S_0 and R_0 are the surface area and the mean curvature of matrix particles respectively, $\alpha_0 = R_0 S_0/3V_0$ is the parameter of non-sphericity of matrix particles.

The probability to find a place for the scaled particle in a HCB matrix is equal to

$$p_0(\lambda_s) = 1 - \eta_0\left(1 + 3\alpha_0\frac{R_1\lambda_s}{R_0} + 3\alpha_0\frac{\lambda_s^2 S_1}{S_0} + \lambda_s^3\frac{V_1}{V_0}\right). \tag{1.30}$$

The corresponding derivatives from (1.30) used for the SPT ansatz are

$$p_0' = -3\eta_0\alpha_0\frac{R_1}{R_0}, \quad p_0'' = -6\eta_0\alpha_0\frac{S_1}{S_0}. \tag{1.31}$$

Similarly, in the case of OHCB matrix one can obtain an expression for the probability $p_0(\lambda_s)$:

$$p_0(\lambda_s) = \exp\left[-\eta_0\left(1 + 3\alpha_0\frac{R_1}{R_0}\lambda_s + 3\alpha_0\frac{S_1}{S_0}\lambda_s^2 + \frac{V_1}{V_0}\lambda_s^3\right)\right] \tag{1.32}$$

as well as the expressions for its derivatives

$$p_0' = -3\eta_0\alpha_0\frac{R_1}{R_0}\phi_0, \quad p_0'' = -3\eta_0\alpha_0\left(2\frac{S_1}{S_0} - 3\eta_0\alpha_0\left(\frac{R_1}{R_0}\right)^2\right)\phi_0. \tag{1.33}$$

Therefore, using (1.10) the coefficients A and B can be derived as

$$\begin{aligned} A &= 3\left[2\alpha_1 + \alpha_0\frac{\eta_0}{(1-\eta_0)}\frac{R_1}{R_0}(1 + 3\alpha_1) + \alpha_0\frac{S_1}{S_0}\frac{\eta_0}{(1-\eta_0)} + 3\alpha_0^2\frac{R_1^2}{R_0^2}\frac{\eta_0^2}{(1-\eta_0)^2}\right], \\ B &= \frac{9}{2}\left(\alpha_1 + \alpha_0\frac{R_1}{R_0}\frac{\eta_0}{1-\eta_0}\right)^2 \end{aligned} \tag{1.34}$$

for a HCB fluid in a HCB matrix and as

$$\begin{aligned} A &= 3\left[2\alpha_1 + \alpha_0\eta_0\frac{R_1}{R_0}(1 + 3\alpha_1) + \alpha_0\frac{S_1}{S_0}\eta_0 + 3\alpha_0^2\frac{R_1^2}{R_0^2}\eta_0^2\right], \\ B &= \frac{9}{2}\left(\alpha_1 + \alpha_0\frac{R_1}{R_0}\eta_0\right)^2 \end{aligned} \tag{1.35}$$

for a HCB fluid in an OHCB matrix.

An accuracy of the approximations proposed in [31] were tested by a comparison with computer simulation data obtained from the grand-canonical Monte Carlo (GCMC) simulations [36]. In this study a model of a HS fluid in a OHCB matrix was investigated. Four different OHCB matrices with parameters presented in Table 1.1 were considered. Using the different approximations the chemical potential depending on the fluid density (packing fraction) is calculated (Fig. 1.1). As one can see at low fluid densities all approximations are correct except the SPT2

Table 1.1 Parameters and characteristics of matrices for the systems A, B, C and D

System	L_0	D_0	η_0	ϕ_0	ϕ	α_0
A	2.0	3.0	0.282	0.754	0.556	1.111
B	3.0	2.0	0.271	0.762	0.493	1.346
C	5.0	2.0	0.099	0.9052	0.781	1.658
D	10.0	1.0	0.167	0.846	0.491	4.125

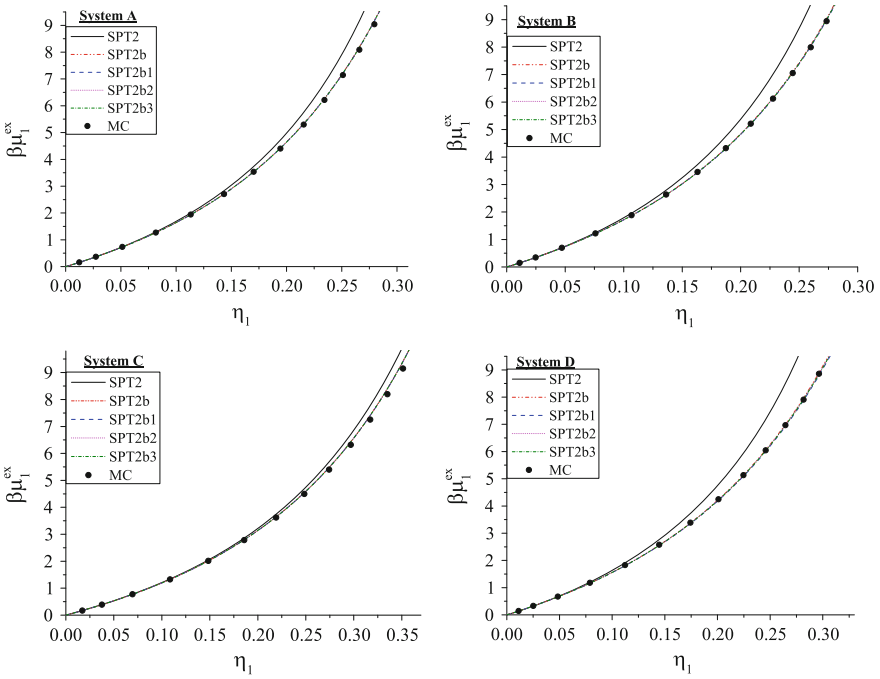

Fig. 1.1 The excess chemical potential $\beta\mu_1^{ex}$ versus the fluid packing fraction η_1 for a HS fluid in random OHCB matrices. The parameters of matrices are presented in Table 1.1. A comparison of the different approximations (*lines*) with the GCMC simulation results (*symbols*)

approach, which overestimates the chemical potential at intermediate densities in a comparison with the GCMC data. On the other hand, the SPT2b approximation improves essentially the results for intermediate fluid densities. In the most considered cases the results of SPT2b coincide with other approximations (SPT2b1, SPT2b2 and SPT2b3) and the observed deviations are comparable with the statistical errors of the simulations (0.5 %). However, as it was shown in [31] in the case of a large difference between the porosities ϕ and ϕ_0, at high fluid densities the approximations SPT2b1, SPT2b2 and SPT2b3 give better results than the SPT2b approach.

1.3 Hard Spherocylinder Fluid in Random Porous Media: SPT with Two Scaling Parameters

Generally, if a shape of hard convex body particles is not strictly specified or it is rather complex, it is acceptable to restrict oneself by one scaling parameter. On the other hand, particles of spherocylindrical shape are characterized only by two measures, i.e. by their length and diameter. Therefore, applying the SPT formalism it is reasonable to change sizes of scaled particle along exactly these two measures. We consider two scaling parameters generalization of the SPT theory for the description of thermodynamic properties of a hard spherocylinder (HSC) fluid in random matrices. We also apply these results to a study of the effect of porous medium on the isotropic-nematic orientational transition appearing in this fluid.

As it was mentioned above a hard spherocylinder system is defined by the volume V, the surface area S and the mean curvature R given by (1.1). According to the general idea of the SPT theory [28, 29, 32] we introduce in a confined HSC fluid an additional hard spherocylinder with the scaling diameter D_s and the scaling length L_s:

$$D_s = \lambda_s D_1, \quad L_s = \alpha_s L_1, \tag{1.36}$$

where D_1 and L_1 are the diameter and the length of fluid spherocylinders respectively. The excess chemical potential for the small scaled particle in a HSC fluid confined in a matrix can be written in the form

$$\begin{aligned}\beta\mu_s^{ex} = &-\ln p_0(\alpha_s,\lambda_s) - \ln\Bigg[1 - \frac{\eta_1}{V_1 p_0(\alpha_s,\lambda_s)}\Big(\frac{\pi}{6}D_1^3(1+\lambda_s)^3 \\ &+ \frac{\pi}{4}D_1^2 L_1(1+\lambda_s)^2(1+\alpha_s) \\ &+ \frac{\pi}{4}D_1 L_1^2(1+\lambda_s)\alpha_s\int f(\Omega_1)f(\Omega_2)\sin\vartheta_{12}d\Omega_1 d\Omega_2\Big)\Bigg],\end{aligned} \tag{1.37}$$

where $\eta_1 = \rho_1 V_1$ is the fluid packing fraction and ρ_1 is the fluid density; $p_0(\alpha_s,\lambda_s)$ is the probability to find a cavity created by a scale particle in the empty matrix and it is defined by the excess chemical potential μ_s^0 of the scale particle in the limit of infinite dilution of a fluid; $\Omega = (\vartheta,\varphi)$ is the orientation of particles defined by the angles ϑ and φ; $d\Omega = \frac{1}{4\pi}\sin\vartheta d\vartheta d\varphi$ is the normalized angle element; ϑ_{12} is the angle between orientational vectors of two molecules; $f(\Omega)$ is the single orientational distribution function normalized in such a way that

$$\int f(\Omega)d\Omega = 1. \tag{1.38}$$

For the large scale particle the excess chemical potential is given by a thermodynamic expression, which can be presented in the form similar to (1.4):

$$\beta\mu_s^{ex} = w(\alpha_s, \lambda_s) + \beta PV_s/p_0(\lambda_s, \alpha_s), \tag{1.39}$$

where $w(\alpha_s, \lambda_s)$ is the following:

$$w(\lambda_s, \alpha_s) = w_{00} + w_{10}\lambda_s + w_{01}\alpha_s + w_{11}\alpha_s\lambda_s + \frac{w_{20}\lambda_s^2}{2}. \tag{1.40}$$

According to the ansatz of SPT theory [28, 29, 32] the coefficients of the expansion (1.40) can be found from the continuity of the excess chemical potential given in (1.37) and (1.39), as well as from the corresponding derivatives $\partial\mu_s^{ex}/\partial\lambda_s$, $\partial\mu_s^{ex}/\partial\alpha_s$, $\partial^2\mu_s^{ex}/\partial\alpha_s\partial\lambda_s$ and $\partial^2\mu_s^{ex}/\partial\lambda_s^2$. As a result one derives the following coefficients

$$w_{00} = -\ln(1 - \eta_1/\phi_0), \tag{1.41}$$

$$w_{10} = \frac{\eta_1/\phi_0}{1 - \eta_1/\phi_0}\left(\frac{6\gamma_1}{3\gamma_1 - 1} - \frac{p'_{0\lambda}}{\phi_0}\right), \tag{1.42}$$

$$w_{01} = \frac{\eta_1/\phi_0}{1 - \eta_1/\phi_0}\left(\frac{3(\gamma_1 - 1)}{3\gamma_1 - 1} + \frac{3(\gamma_1 - 1)^2}{3\gamma_1 - 1}\tau(f) - \frac{p'_{0\alpha}}{\phi_0}\right), \tag{1.43}$$

$$\begin{aligned} w_{11} = \frac{\eta_1/\phi_0}{1 - \eta_1/\phi_0}\Bigg(&\frac{6(\gamma_1 - 1)}{3\gamma_1 - 1} + \frac{3(\gamma_1 - 1)^2\tau(f)}{3\gamma_1 - 1} - \frac{p''_{0\alpha\lambda}}{\phi_0} \\ &+ 2\frac{p'_{0\alpha}p'_{0\lambda}}{\phi_0^2} - \frac{3(\gamma_1 - 1) + 3(\gamma_1 - 1)^2\tau(f)}{3\gamma_1 - 1}\frac{p'_{0\lambda}}{\phi_0} - \frac{6\gamma_1}{3\gamma_1 - 1}\frac{p'_{0\alpha}}{\phi_0}\Bigg) \\ &+ \left(\frac{\eta_1/\phi_0}{1 - \eta_1/\phi_0}\right)^2\left(\frac{6\gamma_1}{3\gamma_1 - 1} - \frac{p'_{0\lambda}}{\phi_0}\right) \\ &\times \left(\frac{3(\gamma_1 - 1)}{3\gamma_1 - 1} + \frac{3(\gamma_1 - 1)^2\tau(f)}{3\gamma_1 - 1} - \frac{p'_{0\alpha}}{\phi_0}\right), \end{aligned} \tag{1.44}$$

$$\begin{aligned} w_{20} = \frac{\eta_1/\phi_0}{1 - \eta_1/\phi_0}\Bigg(&\frac{6(1 + \gamma_1)}{3\gamma_1 - 1} - \frac{12\gamma_1}{3\gamma_1 - 1}\frac{p'_{0\lambda}}{\phi_0} + 2\left(\frac{p'_{0\lambda}}{\phi_0}\right)^2 - \frac{p''_{0\lambda\lambda}}{\phi_0}\Bigg) \\ &+ \left(\frac{\eta_1/\phi_0}{1 - \eta_1/\phi_0}\right)^2\left(\frac{6\gamma_1}{3\gamma_1 - 1} - \frac{p'_{0\lambda}}{\phi_0}\right)^2, \end{aligned} \tag{1.45}$$

where

$$\gamma_1 = 1 + \frac{L_1}{D_1}, \tag{1.46}$$

$$\tau(f) = \frac{4}{\pi}\int f(\Omega_1)f(\Omega_2)\sin\vartheta_{12}d\Omega_1 d\Omega_2. \tag{1.47}$$

If both the scale parameters equal to zero $\alpha_s = \lambda_s = 0$, the probability p_0 is equivalent to the geometrical porosity:

$$\phi_0 = p_0(\alpha_s = \lambda_s = 0), \tag{1.48}$$

and in the case of HSC matrix or overlapping HSC matrix it is defined by the relations (1.26) or (1.27) respectively.

Setting $\alpha_s = \lambda_s = 1$ in the (1.39) leads to the expression similar to (1.9), the chemical potential μ_1^{ex} of a fluid in a matrix. However, now the constants A and B have more general and complicated form

$$\begin{aligned} A(\tau(f)) = 6 &+ \frac{6(\gamma_1-1)^2\tau(f)}{3\gamma_1-1} \\ &- \frac{p'_{0\lambda}}{\phi_0}\left(4+\frac{3(\gamma_1-1)^2\tau(f)}{3\gamma_1-1}\right) - \frac{p'_{0\alpha}}{\phi_0}\left(1+\frac{6\gamma_1}{3\gamma_1-1}\right) \\ &- \frac{p''_{0\alpha\lambda}}{\phi_0} - \frac{1}{2}\frac{p''_{0\lambda\lambda}}{\phi_0} + 2\frac{p'_{0\alpha}p'_{0\lambda}}{\phi_0^2} + \left(\frac{p'_{0\lambda}}{\phi_0}\right)^2, \end{aligned} \tag{1.49}$$

$$\begin{aligned} B(\tau(f)) = &\left(\frac{6\gamma_1}{3\gamma_1-1} - \frac{p'_{0\lambda}}{\phi_0}\right) \\ &\times \left(\frac{3(2\gamma_1-1)}{3\gamma_1-1} + \frac{3(\gamma_1-1)^2\tau(f)}{3\gamma_1-1} - \frac{p'_{0\alpha}}{\phi_0} - \frac{1}{2}\frac{p'_{0\lambda}}{\phi_0}\right), \end{aligned} \tag{1.50}$$

where $p'_{0\lambda} = \frac{\partial p_0(\alpha_s,\lambda_s)}{\partial\lambda_s}, p'_{0\alpha} = \frac{\partial p_0(\alpha_s,\lambda_s)}{\partial\alpha_s}, p''_{0\alpha\lambda} = \frac{\partial^2 p_0(\alpha_s,\lambda_s)}{\partial\alpha_s\partial\lambda_s}, p''_{0\lambda\lambda} = \frac{\partial^2 p_0(\alpha_s,\lambda_s)}{\partial\lambda_s^2}$ are the corresponding derivatives at $\alpha = \lambda = 0$. Also the probe particle porosity ϕ can be obtained from

$$\phi = p_0(\alpha_s = \lambda_s = 1). \tag{1.51}$$

In order to derive expressions for the chemical potential we repeat the calculations presented in the previous section. Using the Gibbs-Duhem equation we get an expression for the compressibility in the form (1.12). After integration of this expression over the fluid density we obtain the excess chemical potential μ_1^{ex} and the pressure of a fluid in the form similar to the SPT2 approximation (1.13)–(1.14). On the basis of SPT2 result we construct the SPT2b approximation in the form (1.15) to (1.16). Following to the the scheme presented in the previous section we also derive the expressions for the SPT2b1, SPT2b2 and SPT2b3 approximations in the form like (1.18)–(1.19), (1.21)–(1.22) and (1.23)–(1.24) respectively. The only

difference in the new expressions of the chemical potential in a comparison with ones obtained in the previous section is an additional entropic term $\sigma(f)$:

$$\sigma(f) = \int f(\Omega) \ln f(\Omega) d\Omega. \tag{1.52}$$

As an example we present here the expression for the chemical potential of a fluid confined in a matrix using the SPT2b approximation:

$$\begin{aligned}\beta(\mu_1^{ex} - \mu_1^0)^{SPT2b} = \sigma(f) - \ln(1 - \eta_1/\phi) + (1 + A(\tau(f)))\frac{\eta_1/\phi_0}{1 - \eta_1/\phi_0} \\ + \frac{1}{2}(A(\tau(f)) + 2B(\tau(f)))\frac{(\eta_1/\phi_0)^2}{(1 - \eta_1/\phi_0)^2} \\ + \frac{2}{3}B(\tau(f))\frac{(\eta_1/\phi_0)^3}{(1 - \eta_1/\phi_0)^3}.\end{aligned} \tag{1.53}$$

From the thermodynamic relationship

$$\frac{\beta F}{V} = \beta\mu_1\rho_1 - \beta P \tag{1.54}$$

one can obtain the expression for the free energy. Within the SPT2b approximation the free energy of a confined fluid is the following

$$\begin{aligned}\beta V^{-1} F^{SPT2b} = \rho_1\sigma(f) + \rho_1(\ln(\Lambda_1^3\rho_1) - 1) + \beta\mu_1^0\rho_1 - \rho_1 \ln(1 - \eta_1/\phi) \\ + \frac{\rho_1\phi}{\eta_1}\ln(1 - \eta_1/\phi) - \frac{\rho_1\phi_0}{\eta_1}\ln(1 - \eta_1/\phi_0) \\ + \rho_1\frac{A(\tau(f))}{2}\frac{\eta_1/\phi_0}{1 - \eta_1/\phi_0} + \rho_1\frac{B(\tau(f))}{3}\left(\frac{\eta_1/\phi_0}{1 - \eta_1/\phi_0}\right)^2.\end{aligned} \tag{1.55}$$

Now we return to the orientational distribution function $f(\Omega)$ introduced in the beginning of this section. Distribution function $f(\Omega)$ can be determined from a minimization of the free energy with respect to variations in this distribution. This procedure leads to the nonlinear integral equation

$$\ln f(\Omega_1) + 1 + C\int f(\Omega_2)\sin\vartheta_{12} d\Omega_2 = 0, \tag{1.56}$$

where

$$C = \frac{\eta_1/\phi_0}{1-\eta_1/\phi_0}\left[\frac{3(\gamma_1-1)^2}{3\gamma_1-1}\left(1-\frac{p'_{0\lambda}}{2\phi_0}\right)\right. \\ \left. + \frac{\eta_1/\phi_0}{(1-\eta_1/\phi_0)}\frac{(\gamma_1-1)^2}{3\gamma_1-1}\left(\frac{6\gamma_1}{3\gamma_1-1}-\frac{p'_{0\lambda}}{\phi_0}\right)\right]. \tag{1.57}$$

The (1.56) should be solved together with the normalization condition (1.38). The solution of the (1.56) can be calculated numerically using an iteration procedure according to the algorithm proposed in [37]. We should note that the (1.56) for the singlet distribution function $f(\Omega)$ has the same structure as the corresponding equation obtained by Onsager [38] for the hard spherocylinder fluid in the limit $L \to \infty$, $D_1 \to 0$, while the dimensionless density of fluid $c = \frac{1}{4}\pi L_1^2 D_1 \rho_1$ is fixed. Therefore, in the Onsager limit one has

$$C \to c = \frac{1}{4}\pi L_1^2 D_1 \rho_1. \tag{1.58}$$

This result within the framework of the SPT theory was generalized for a HSC fluid with the finite value of L_1 and D_1 [39, 40], and in this case

$$C = \frac{\eta_1}{1-\eta_1}\left[\frac{3(\gamma_1-1)^2}{3\gamma_1-1}+\frac{\eta_1}{1-\eta_1}\frac{6\gamma_1(\gamma_1-1)^2}{(3\gamma_1-1)^2}\right]. \tag{1.59}$$

It is not difficult to show that the expression (1.59) corresponds to the bulk case ($\phi_0 = 1, p'_{0\lambda} = 0$) of our result (1.57).

From the bifurcation analysis of (1.56) it is found that this equation has two characteristic points c_i and c_n [41]. For the Onsager model in the bulk [41, 42]

$$c_i = 3.290, \quad c_n = 4.191, \tag{1.60}$$

where c_i corresponds to high densities of stable isotropic fluid and c_n is related with the minimal density of stable orientational ordering, i.e. a nematic state of fluid.

In the presence of a porous medium for the Onsager model we obtain

$$c_i/\phi_0 = 3.290, \quad c_n/\phi_0 = 4.191. \tag{1.61}$$

It means that the isotropic-nematic phase transition in the presence of a matrix shifts to lower densities of a fluid.

For finite values of L_1 and D_1 we can put

$$C_i = 3.290, \quad C_n = 4.191, \tag{1.62}$$

where C_i and C_n are defined from (1.57). The values in (1.62) define the isotropic-nematic phase diagram for a HSC fluid in a matrix depending on the ratio L_1/D_1 and the parameters of a matrix.

As an example we consider a porous medium formed by a HS matrix. The probability to find scaled spherocylinder in an empty HS matrix is equal to

$$p_0(\alpha_s, \lambda_s) = 1 - \eta_0 \frac{1}{V_0} \frac{\pi}{2} \left[\frac{1}{3} (D_0 + \lambda_s D_1)^3 + \frac{1}{2} \alpha_s L_1 (D_0 + \lambda_s D_1)^2 \right]. \tag{1.63}$$

From (1.63) one can find the derivatives needed for the description of thermodynamic properties of a confined fluid:

$$p'_{0\alpha} = -3 \frac{D_1}{D_0} \eta_0, \quad p'_{0\alpha} = -\frac{3}{2} \eta_0 \frac{L_1}{D_0}, \quad p''_{0\alpha\lambda} = -3\eta_0 \frac{L_1}{D_0} \frac{D_1}{D_0}, \quad p''_{0\lambda\lambda} = -6\eta_0 \frac{D_1^2}{D_0^2}, \tag{1.64}$$

where η_0 is the packing fraction of HS matrix particles. The probe particle porosity in this case is equal to [32]

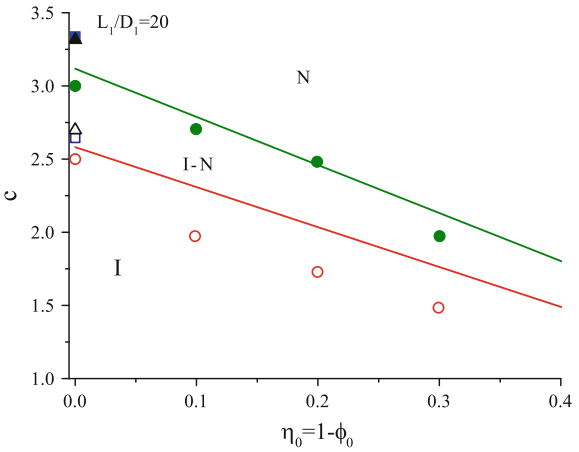

Fig. 1.2 Coexistence lines of isotropic-nematic phases of a hard spherocylinder fluid in a hard sphere matrix for $L_1/D_1 = 20$ and $D_0 = L_1$ presented as a dependence of the spherocylinder fluid density $c = \frac{1}{4}\pi\rho_1 L_1^2 D_1$ on the matrix packing fraction η_0. The GEMC simulation results taken from [7] are shown as *circles*, from [43] are shown as *squares* and *triangles* (GDI). The isotropic phase are denoted by open symbols and the nematic phase—by filled symbols. Solid lines corresponds to the SPT theory. The notations "I" and "N" mean isotropic and nematic phases respectively

$$\phi = (1-\eta_0)\exp\left[-\frac{\eta_0}{1-\eta_0}\frac{D_1}{D_0}\left(\frac{3}{2}(\gamma_1+1)+3\gamma_1\frac{D_1}{D_0}\right)-\frac{\eta_0^2}{(1-\eta_0)^2}\frac{9}{2}\gamma_1\frac{D_1^2}{D_0^2}\right.$$
$$\left.-\frac{\eta_0}{(1-\eta_0)^3}(3\gamma_1-1)\frac{1}{2}\frac{D_1^3}{D_0^3}(1+\eta_0+\eta_0^2)\right]. \tag{1.65}$$

The analysis of the phase diagrams of a fluid in a matrix [32] obtained according to (1.57) and (1.62) shows that the isotropic-nematic phase coexistence shifts to smaller densities with decreasing of the value of L_1/D_1 as well as with decreasing of the matrix porosity ϕ_0. In Fig. 1.2 one can observe how the matrix porosity affects the phase coexistence in the case of the HSC fluid with $L_1/D_1 = 20$ and the HS matrix with $L_1/D_0 = 1$. For comparison in this figure it is also presented the results of computer simulation of Schmidt and Dijkstra [7] obtained by the method of Gibbs ensemble Monte Carlo (GEMC). For the bulk case ($\eta_0 = 0$) the results of Bolhuis and Frenkel [43] are shown in Fig. 1.2 as well. These results were obtained using the common GEMC method and GEMC combined with the modified Gibbs-Duhem integration (GDI) method. As one can see in Fig. 1.2 our theory overestimates the effect of porous medium, especially it is noticeable for the isotropic branch of phase coexistence. On the other hand, the nematic branch looks rather satisfactory.

We should note that for isotropic-nematic coexistence lines can also be found from the condition of thermodynamic equilibrium. According to this the isotropic and nematic phases have the same pressure and the same chemical potential:

$$P_i(c_i) = P_n(c_n), \quad \mu_i(c_i) = \mu_n(c_n). \tag{1.66}$$

In [41] it was shown for the Onsager model in the bulk case that the results obtained from bifurcation analysis and from the thermodynamic consideration coincide exactly. Evidently, we can expect the same for the Onsager model in the case of the porous medium presence. We observed in [32] that for the finite value of L_1/D_1 there is some deviation between the results obtained from the thermodynamic and bifurcation analysis, which increases slightly with increasing of the ratio L_1/D_1.

1.4 Generalization of Van der Waals Equation for Anisotropic Fluid in Random Porous Media

It is well established that the short-range order in simple and molecular liquids is determined by the repulsive part of intermolecular interaction [33, 34]. Such a short-range structure is essentially related to the packing of hard core particles, which can be modeled by hard spheres (HS) in the case of simple fluid or hard

convex bodies (HCB) system in the case of molecular fluid. Similar to the bulk case [33, 34, 44] the results obtained from the SPT theory for HS and HCB fluids confined in random matrices can be used as the reference system within the perturbation theory of fluids. In this section as the first step we consider the possibility of an extension of the Van der Waals Equation of state to a simple and anisotropic molecular fluid in a random porous medium.

Considering the case of a simple fluid with a pair potential of interaction, which consists of a HS repulsive and an attractive parts, we start from the well-known Kac potential [45, 46]

$$U^{att}(r) = \gamma^3 U(\gamma r), \tag{1.67}$$

where r is a distance between two particles. In the same way as for a bulk fluid in the limit $\gamma \to 0$ the pressure of a confined fluid can be presented in the form [44, 45]

$$\frac{\beta P}{\rho_1} = \left(\frac{\beta P}{\rho_1}\right)_{HS} - 12a\eta_1\beta, \tag{1.68}$$

where $\left(\frac{\beta P}{\rho_1}\right)_{HS}$ is a contribution of a HS interaction, which can be obtained from (1.16) within the SPT2b approximation, and $\beta = 1/k_B T$. Therefore, a HS fluid confined in a random matrix is taken as a reference system. The second term in (1.68) is a contribution of the attractive interaction defined by the constant a, which can be calculated from the following expression:

$$a = -\frac{1}{\phi_0 D_1^3}\int_0^\infty \gamma^3 U(\gamma r) r^2 dr, \tag{1.69}$$

where the factor $1/\phi_0$ excludes the volume occupied by matrix particles, since this volume does not contribute to the fluid attraction. We also introduce a size of hard core of fluid particles D_1, which means a diameter of HS particles.

As an example, we substitute an attractive pair potential $U^{att}(r)$ with the Lennard-Jones potential [44] in the form

$$U^{att}(r) = \begin{cases} 4\varepsilon_1\left[\left(\frac{D_1}{r}\right)^{12} - \left(\frac{D_1}{r}\right)^6\right], & r \geq D_1 \\ 0, & r < D_1 \end{cases}. \tag{1.70}$$

Using the Gibbs-Duhem relationship one can derive the expression of chemical potential from (1.68). Having the analytical expressions for the equation of state and the chemical potential one can build the liquid-vapour phase diagram in coordinates $\eta_1 - T^*$, where T^* is dimensionless temperature $T^* = kT/\varepsilon_1 = 1/\beta\varepsilon_1$.

In Fig. 1.3 the liquid-vapour coexistence curves are presented for a simple fluid in HS matrices of the different porosities ϕ_0. One can see that the coexistence curves shift toward lower temperatures and lower fluid densities if the matrix

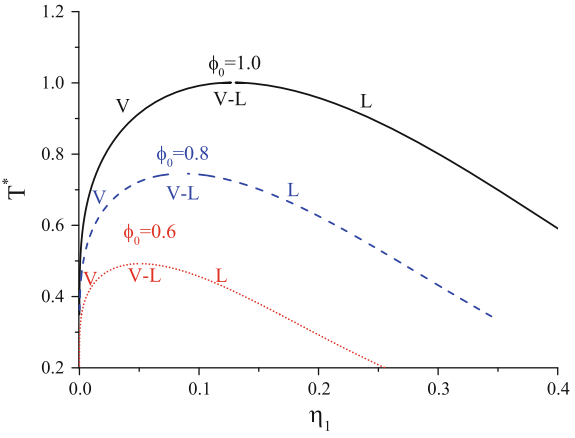

Fig. 1.3 Liquid-vapour coexistence curves ($T^* = kT/\varepsilon_1$ is a reduced temperature, η_1 is a fluid packing fraction) calculated from a generalized Van der Waals (1.68) for a simple fluid in a HS matrix of the different porosity ϕ_0

porosity decreases. Therefore, the critical density η_c and critical temperature T_c^* decrease with matrix porosity decreasing. This behavior is very common for fluids in random confinements [11, 25, 47].

It is worth mentioning that the interpretation of experimental results for the phase behaviour of fluid in random porous media [48] is enough controversial. From one point of view a fluid in a quenched disorder or in a random matrix can be considered as experimental realization of the random-field Ising model [49]. Within this model the random field describes the spatially varying preference of the porous media for different fluid phases. From the other point of view the behaviour of a fluid in a porous medium can be described in terms of the wetting states of the two phases in a single pore of ideal geometry [50]. We do not focus here specially on the influence of porous media on the behaviour of fluid near the critical point. However, since the conventional Van der Waals Equation of state for the bulk fluid gives the mean field description, one can consider that our analog of the Van der Waals equation for a fluid in a random porous matrix leads to the same critical exponents.

A description of molecular fluids requires a corresponding generalization of (1.68), which takes into account an anisotropic nature of the interaction between molecules. An extension of the expression (1.68) to the case of a system non-spherical particles with orientations starts from the following

$$\frac{\beta P}{\rho_1} = \left(\frac{\beta P}{\rho_1}\right)_{HCB} - 12a\eta_1\beta, \tag{1.71}$$

where $\left(\frac{\beta P}{\rho_1}\right)_{HCB}$ is the hard convex body contribution of the reference system. In our study the HCB particles are considered as hard spherocylinders (HSC). Also we restrict ourselves to the approximation SPT2b.

The attraction term depends on the constant a which is expressed in the general form as

$$a = -\frac{1}{\phi_0 V_1}\int f(\Omega_1) f(\Omega_2) U^{att}(r_{12}\Omega_1\Omega_2) d\bar{r}_{12} d\Omega_1 d\Omega_2, \tag{1.72}$$

where V_1 is the volume of a spherocylindrical molecule. One can see that the attractive pair potential $U^{att}(r_1\Omega_1\Omega_2)$ in (1.72) is orientational dependent. Therefore, except the anisotropic repulsive interaction of HSC particles the attractive part of intermolecular interaction is anisotropic as well. We introduce an orientational dependence for the potential U^{att} by modifying the Lennard-Jones potential in the following way

$$U^{att}(r_{12}\Omega_1\Omega_2) = U_{LJ}\left(\frac{\sigma(\Omega_1\Omega_2\Omega_r)}{r_{12}}\right)[1 + \chi P_2(\cos\vartheta_{12})], \tag{1.73}$$

$$U_{LJ}\left(\frac{\sigma(\Omega_1\Omega_2\Omega_r)}{r_{12}}\right) = \begin{cases} 4\varepsilon_1\left[\left(\frac{\sigma(\Omega_1\Omega_2\Omega_r)}{r_{12}}\right)^{12} - \left(\frac{\sigma(\Omega_1\Omega_2\Omega_r)}{r_{12}}\right)^{6}\right], & r_{12} \geq \sigma(\Omega_1\Omega_2\Omega_r) \\ 0, & r_{12} < \sigma(\Omega_1\Omega_2\Omega_r) \end{cases} \tag{1.74}$$

where $P_2(\cos\vartheta_{12}) = \frac{1}{2}(3\cos^2\vartheta_{12} - 1))$ is the second Legendre polynomial, the relative orientation ϑ_{12} corresponds to the angle between the principal axes of the two molecules. $\sigma(\Omega_1\Omega_2\Omega_r)$ is the contact distance between molecules, and it depends on the orientations of two interacting molecules as well as on the orientation of a distance vector $\vec{r}_{12}$ between their centers. It is worth noting that in the case of the repulsive part of the potential is spherically symmetric (σ is fixed) the expression for the potential (1.73) reduces to the Maier-Saupe potential [51].

One can see that (1.73) is a sum of two Lennard-Jones potentials, where the first one is related to the isotropic attraction and another one corresponds to the anisotropic attraction. The ratio of the well depths of these two potentials $\chi = \varepsilon_2/\varepsilon_1$ specifies a rate of anisotropy in the attraction of the resulted potential (1.73).

Following the traditional scheme [52], taking into account that $d\bar{r} = r^2 dr d\Omega_r$ and using a dimensionless intermolecular distance $r^* = r/\sigma(\Omega_1\Omega_2\Omega_r)$ one obtains

$$\begin{aligned} a = -\frac{1}{\phi_0 V_1}\int d\Omega_1 d\Omega_2 f(\Omega_1) f(\Omega_2)[1 + \chi P_2(\cos\vartheta_{12})] \\ \times\ V_1^{exc}(\Omega_1\Omega_2) 3\int_0^\infty r^{*2} dr^* \beta U_{LJ}(r^*), \end{aligned} \tag{1.75}$$

where

$$V_{exc}(\Omega_1\Omega_2) = \frac{1}{3}\int d\Omega_r [\sigma(\Omega_1\Omega_2\Omega_r)]^3 \tag{1.76}$$

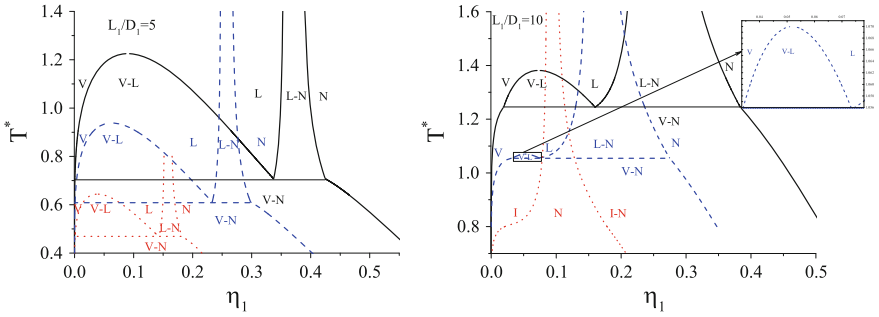

Fig. 1.4 The temperature-density phase diagram ($T^* = kT/\varepsilon_1$ is a reduced temperature, η_1 is a fluid packing fraction) calculated from the generalized Van der Waals (1.71) for the attractive spherocylinder fluid in a bulk and in HS matrices of porosity $\phi_0 = 1.0$ (*solid lines*), $\phi_0 = 0.8$ (*dashed lines*) and $\phi_0 = 0.6$ (*dotted lines*). The *horizontal lines* correspond to the vapour-liquid-nematic three-phase coexistence separating the vapour-liquid (VL), liquid-nematic (L-N) and vapour-nematic (V-N) regions. Two ratios of length to diameter of spherocylinder molecules are considered: $L_1/D_1 = 5$ (*left panel*) and $L_1/D_1 = 10$ (*right panel*)

is excluded volume formed by two hard spherocylinders with the orientations Ω_1 and Ω_2.

In order to study the anisotropy effect only in the repulsive part of intermolecular interaction, we put $\chi = 0$. For this case the phase diagrams for the system of HSC fluid with $L_1/D_1 = 5$ and $L_1/D_1 = 10$ in the bulk ($\phi_0 = 1.0$) and in the porous matrices ($\phi_0 < 1.0$) are presented in Fig. 1.4. Similar as it was shown for the bulk [52], for our model three regions of liquid phase equilibria are apparent. At low and intermediate densities the phase equilibrium between vapour (V) and isotropic liquid (L) states is observed. The coexistence region between the isotropic liquid (L) and the anisotropic nematic (N) states appears at high densities. The isotropic-nematic (I-N) transition is related mainly to the non-spherical shape of molecules, hence the position of this transition does not change with the temperature. In the high-temperature limit the liquid-nematic (L-N) transition vanishes and the system tends to that for a HSC fluid in a matrix. In contrast to this the temperature decrease leads to the L-N region becomes broader. At sufficiently low temperatures, the region merges into the continuous vapour-liquid region at the vapour-liquid-nematic (V-L-N) triple point. Below the triple point temperature only the vapour-nematic (V-N) coexistence is seen. In the porous matrix presence all the phase diagrams shift to the region of lower temperatures and lower densities similar as it was observed in the case of simple fluids (Fig. 1.3).

With increasing of the ratio L_1/D_1 to 10 the liquid-nematic region becomes much more extensive (Fig. 1.4). The vapour-liquid region for $L_1/D_1 = 10$ is essentially narrower than in the case of $L_1/D_1 = 5$, while the liquid-nematic region covers a wide range of densities. As one can see in Fig. 1.4 a porous medium for $L_1/D_1 = 10$ can modify the phase behaviour of a fluid qualitatively. For instance, for the porosity $\phi_0 = 0.8$ the vapour-liquid coexistence region in the case of $L_1/D_1 = 10$ is very small. Therefore, for such a fluid in matrices with porosities lower than $\phi_0 = 0.8$

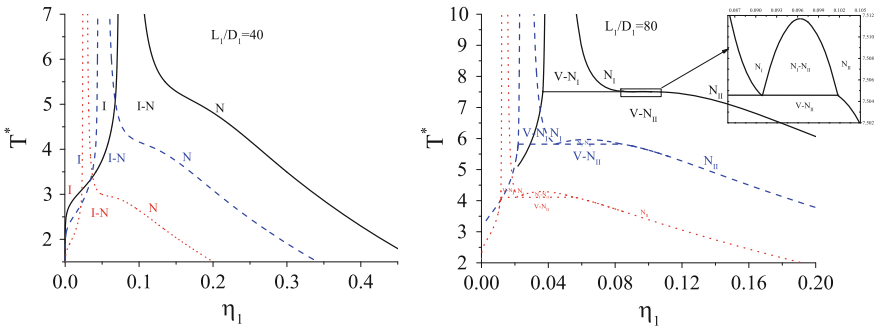

Fig. 1.5 The same as in Fig. 1.4, but for the ratios of length to diameter of spherocylinder molecules $L_1/D_1 = 40$ (*left panel*) and $L_1/D_1 = 80$ (*right panel*). For $L_1/D_1 = 80$ the coexisting region of nematic vapour and nematic liquid $(N_I - N_{II})$ with corresponding critical point is observed. The horizontal lines correspond to the vapour-nematic-nematic three phase coexistence, which separates the vapour-nematic $(V - N_I)$, nematic I-nematic II $(N_I - N_{II})$ and vapour-nematic II $(V - N_{II})$ regions

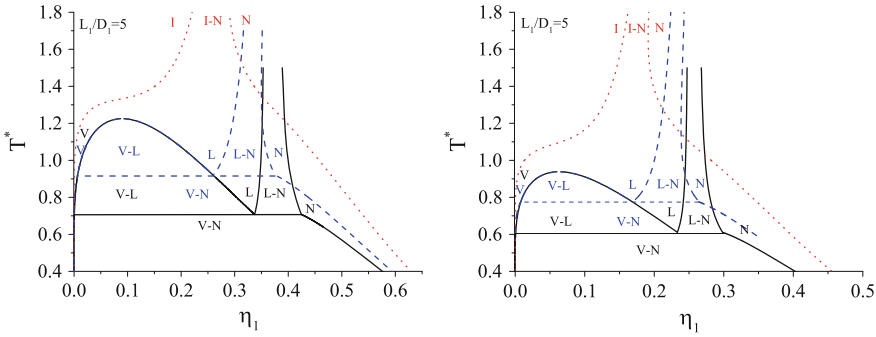

Fig. 1.6 The temperature-density phase diagram ($T^* = kT/\varepsilon_1$ is a reduced temperature, η_1 is a fluid packing fraction) calculated from the generalized Van der Waals (1.69) for the spherocylinder fluid with $L_1/D_1 = 5$ in a bulk (*left panel*) and in a HS matrix of porosity $\phi = 0.8$ (*right panel*). The different anisotropic rates of the attractive potential are considered: $\chi = 0.0$ (*solid lines*), $\chi = 0.1$ (*dashed lines*) and $\chi = 0.4$ (*dotted lines*)

the vapour-liquid coexistence region can disappear completely. Such a situation is observed for $\phi_0 = 0.6$ in Fig. 1.4.

It was also observed that for considerably high values of $L_1/D_1 = 40$ the vapour-liquid coexistence region disappears even in the bulk and the presence of porous medium for these cases does not change this (Fig. 1.5, left panel). Only the isotropic-nematic transition (I-N) is observed for the ratio $L_1/D_1 = 40$. One can see that the porosity decrease leads to the narrowing of the I-N region and it shifts to the lower densities. Since in the Onsager limit $L_1 \to \infty$, $D_1 \to 0$ the isotropic-nematic transition shifts to the lower densities we can expect an appearance of vapour-liquid coexistence in nematic region. Such a situation is observed for $L_1/D_1 = 80$ and it is

presented in Fig. 1.5 (right panel). It is seen that below the triple point temperature of vapour-nematic-nematic transition there is a relatively broad region of V-N coexistence. A decrease of the matrix porosity causes the vapour-nematic region to be more pronounced.

Finally, we focus on the effect of anisotropic attractive interaction on the fluid phase behaviour in a random confinement. The temperature-density projection of the phase behaviour in the case of $L_1/D_1 = 5$ spherocylinder fluid with the different rates of anisotropic attractive interactions χ is presented in Fig. 1.6. As it can be expected the introduction of the anisotropic attractive interaction enhances an ability of the fluid to form orientationally ordered states. The liquid-nematic region broadens out significantly if χ increases, while the vapour-liquid coexistence curve remains unchanged. As a consequence, one can see an increase of the vapour-liquid-nematic triple point. For sufficiently large anisotropy ($\chi = 0.4$) the triple and critical points merge, and as a result only the I-N phase behaviour is found. The presence of porous medium as usually shifts the phase diagram to lower densities and temperatures. Although quantitatively the phase behaviour in the bulk (Fig. 1.6, left panel) and in the presence of porous medium with the porosity $\phi_0 = 0.8$ (Fig. 1.6, right panel) are practically the same.

1.5 Conclusions

The development and the application of the scaled particle theory (SPT) for a study of the thermodynamic properties of molecular liquids in random porous media are reviewed in this chapter. Within the proposed approach a series of different approximations are considered and tested by a comparison with computer simulations. It is shown that the SPT2b approximation fits the simulation results with a good accuracy at low and intermediate fluid densities. The SPT2b1 approximation improves the description at high densities and for the case when sizes of fluid and matrix particles are comparable. For a hard spherocylinder fluid confined in a random matrix the SPT2 approach is extended with a use of two scaling parameters. The results obtained for a hard spherocylinder fluid with two scaling parameters make it possible to study the effect of a porous medium on the isotropic-nematic phase transition. The proposed theory predicts that this transition is of the first order and a decrease of porosity shifts the phase diagrams toward lower fluid densities and temperatures. This prediction is supported by computer simulations [7] and also at least for enough large pores by experimental results [53, 54].

We have demonstrated that the results obtained within the framework of the SPT theory for a system of hard convex body fluid and in particular for a hard spherocylinder fluid can be used as a reference system for an extension of the Van der Waals equation of state to the case of molecular anisotropic fluid in a random porous matrix. Starting from this generalization the Van der Waals equation has made it possible to examine the evolution of vapour-liquid-nematic phase equilibrium depending on the anisotropy of fluid molecules and the porosity of a

random confinement. As it is known [33, 34] the principal defect of the Van der Waals equation is related with a neglect of a fluid structure. Recently [55], we applied the Barker-Henderson perturbation theory [44] for the description of the liquid-vapour phase transition of a simple fluid in a random matrix. The pair distribution function of a hard sphere fluid in a porous medium needed for this theory was taken from numerical calculations of the replica Ornstein-Zernike equations [8, 9, 14, 15]. However, it is observed that the effect of porous medium on the vapour-liquid phase diagram qualitatively comparable with the prediction obtained from the Van der Waals equation. We plan in future to generalize the Barker-Henderson perturbation theory for anisotropic molecular fluids in random porous media.

Another way of a development of the presented theory is related to taking into account of association effects in molecular fluids confined in random porous media. Recently [47], within the framework of the SPT theory we have obtained the analytical expression for the contact value of a pair distribution function of a hard sphere fluid in random matrices. This allowed us to apply the thermodynamic perturbation theory [56, 57] to the treatment of association effects and to construct the phase diagrams of network-forming fluids confined in random matrices. We hope to generalize this approach for molecular anisotropic fluids in random porous media as well.

The developed theory opens new possibilities for the modeling of porous media. Within the framework of the SPT theory a porous medium can be presented as quenched HCB or OHCB particles, thus one can get a description of fluids in wider range of porous structures than those considered in other studies before. However, we should note that a structure of real porous materials can be much more complicated. As it was noted in [1], sometimes the simulation and theory can be used to study the behaviour of adsorbates confined in hypothetical porous materials that do not necessarily correspond to real materials. In order to establish the relation between such simple models of porous medium and more realistic ones we can use the morphological principle of mapping between the thermodynamic properties of a fluid in various matrices [25]. According to this principle the fluid in two different matrices has the same thermodynamic properties if the both matrices have the same probe particle porosity ϕ, the specific pore area s, the mean curvature and the Gaussian curvature. It was shown in [25] that these four morphological measures of a porous medium is enough to make a prediction of the thermodynamic properties of a confined fluid.

Finally, we should emphasize that in this review we focus on the consideration of the effect on fluids caused by porous media exceptionally with a random structure. However, major conclusions made for the case of random porous materials are valid for the case of regular porous materials as well, at least for materials with a high porosity. An understanding of the effect of a non-regular porous structure on confined fluid in a comparison with ordered porous materials needs deeper analysis and it will be studied elsewhere.

References

1. L.D. Gelb, K.E. Gubbins, R. Radhakrishnan, M. Sliwinska-Bartkowiak, Rep. Prog. Phys. **62**, 1573 (1999)
2. C.M. Lastoskie, K.E. Gubbins, Adv. Chem. Eng **28**, 203 (2001)
3. P.A. Monson, Adsorption **11**, 29 (2005)
4. P.A. Monson, J. Chem. Phys **128**, 084701 (2008)
5. Q.-T. Doan, G. Lefevre, O. Hurisse, F.-X. Coudert, Mol. Simulat. **40**, 16 (2014)
6. J. Ilnytskyi, S. Sokolowski, O. Pizio, Phys. Rev. E **59**, 4161 (1999)
7. M. Schmidt, M. Dijkstra, J. Chem. Phys. **121**, 12067 (2004)
8. W.G. Madden, E.D. Glandt, J. Stat. Phys. **51**, 537 (1988)
9. J.A. Given, G. Stell, J. Chem. Phys. **97**, 4573 (1992)
10. T. Patsahan, A. Trokhymchuk, M. Holovko, J. Mol. Liq. **92**, 117 (2001)
11. T. Patsahan, A. Trokhymchuk, M. Holovko, J. Mol. Liq. **105**, 227 (2003)
12. M. Schmidt, Phys. Rev. E **66**, 041108 (2002)
13. M. Schmidt, J. Phys.: Condens. Matter **17**, S3481 (2005)
14. M.L. Rosinberg, C. Caccamo, J.P. Hansen, G. Stell (eds.), *New Approaches to Problems in Liquid State Theory. NATO Science series C*, vol. 529 (Kluwer Dordrecht (Holland), 1999), pp. 245–278
15. O. Pizio, M. Borowko (eds.), *Computational Methods in Surface and Colloidal Science. Surfactant Science Series*, vol. 89 (Kluwer, Marcell Deker, New York 2000), p. 293
16. A.D. Trokhymchuk, O. Pizio, M.F. Holovko, S. Sokolowski, J. Phys. Chem. **100**, 17004 (1996)
17. A.D. Trokhymchuk, O. Pizio, M.F. Holovko, S. Sokolowski, J. Chem. Phys. **106**, 200 (1997)
18. M. Holovko, W. Dong, J. Phys. Chem B **113**, 6360 (2009)
19. W. Chen, W. Dong, M. Holovko, X.S. Chen, J. Phys. Chem. B **114**, 1225 (2010)
20. T. Patsahan, M. Holovko, W. Dong, J. Chem. Phys. **134**, 074503 (2011)
21. H. Reiss, H.L. Frisch, J.L. Lebowitz, J. Chem. Phys. **31**, 369 (1959)
22. H. Reiss, H.L. Frisch, E. Helfand, J.L. Lebowitz, J. Chem. Phys. **32**, 119 (1960)
23. J.L. Lebowitz, E. Helfand, E. Praestgaard, J. Chem. Phys. **43**, 774 (1965)
24. M. Holovko, T. Patsahan, W. Dong, Condens. Matter Phys. **15**, 23607 (2012)
25. M. Holovko, T. Patsahan, W. Dong, Pure Appl. Chem. **85**, 115 (2013)
26. R.M. Gibbons, Mol. Phys. **17**, 81 (1969)
27. T. Boublik, Mol. Phys. **27**, 1415 (1974)
28. M.A. Cotter, D.E. Martire, J. Chem. Phys. **52**, 1970 (1909)
29. M.A. Cotter, Phys. Rev. A **10**, 625 (1974)
30. G. Lasher, J. Chem. Phys. **53**, 4141 (1970)
31. M. Holovko, V. Shmotolokha, T. Patsahan, J. Mol. Liq. **189**, 30 (2014)
32. M. Holovko, V. Shmotolokha, T. Patsahan, (in preparation)
33. I.R. Yukhnovskyi, M.F. Holovko, *Statistical theory of Classical Equilibrium Systems* (Naukova Dumka, Kyiv, 1980)
34. J.P. Hansen, I.R. McDonald, *Theory of Simple Liquids* (Academic Press, London, 2006)
35. C.G. Gray, K.E. Gubbins, *Theory of Molecular Fluids* (Clarendon Press, Oxford, 1984)
36. D. Frenkel, B. Smith, *Understanding Molecular Simulations* (Academic, San Diego, 1995)
37. J. Herzfeld, A.E. Berger, J.W. Wingate, Macromolecules **17**, 1718 (1984)
38. L. Onsager, Ann. N. Y. Acad. Sci. **51**, 627 (1949)
39. M. Cotter, D.C. Wacker, Phys. Rev. A **18**, 2669 (1978)
40. R. Tuinier, T. Taniguchi, H.H. Wensink, Eur. Phys. J. E **23**, 355 (2007)
41. R.F. Kayser Jr., H.J. Raveche, Phys. Rev. A **17**, 2067 (1978)
42. G.J. Vroege, H.N.W. Lekkerkerker, Rep. Prog. Phys. **55**, 1241 (1992)
43. P. Bolhuis, D. Frenkel, J. Chem. Phys. **107**, 666 (1997)
44. J.A. Barker, D. Henderson, Rev. Mod. Phys. **48**, 587 (1976)
45. M. Kac, G.E. Uhlenbeck, P.C. Hammer, J. Math. Phys. **4**, 216 (1963)

46. J.L. Lebowitz, O. Penrose, J. Math. Phys. **7**, 98 (1966)
47. Y.V. Kalyuzhnyi, M. Holovko, T. Patsahan, P. Cummings, J. Phys. Chem. Lett. **5**, 4260 (2014)
48. A.P.Y. Wong, S.B. Kim, W.J. Goldburg, M.H.W. Chan. Phys. Rev. Lett. **70**, 954 (1993)
49. F. Brochard, P.G. de Gennes, J. Phys. Lett (Paris) **44**, 785 (1983)
50. L. Monette, A. Liu, G.S. Grest, Phys. Rev. A. **46**, 7664 (1992)
51. W. Maier, A. Saupe, Z. Naturforsch **14a**, 882 (1959)
52. M. Franco-Melgar, A.J. Haslam, G. Jackson, Mol. Phys. **107**, 2329 (2009)
53. M.D. Dadmun, M. Muthukumar, J. Chem. Phys. **98**, 4850 (1993)
54. G.S. Iannacchione, S. Qian, D. Finotello, F.M. Aliev, Phys. Rev. E **56**, 554 (1997)
55. M. Holovko, T. Patsahan, V. Shmotolokha, Cond. Matter Phys. **18**, 13607 (2015)
56. M.S. Wertheim, J. Stat. Phys. **35**, 19 (1984), **35**, 34 (1984)
57. M.S. Wertheim, J. Stat. Phys. **42**, 459 (1986)